



Long noncoding RNA *MIR31HG* is a *bona fide* prognostic marker with colorectal cancer cell-intrinsic properties

Peter W. Eide ^{1,2,3}, Ina A. Eilertsen ^{1,2,3}, Anita Sveen^{1,2,3} and Ragnhild A. Lothe^{1,2,3}

¹Department of Molecular Oncology, Institute for Cancer Research, Oslo University Hospital, Oslo, Norway

²K.G.Jebsen Colorectal Cancer Research Centre, Oslo University Hospital, Oslo, Norway

³Institute for Clinical Medicine, University of Oslo, Oslo, Norway

Elevated miR-31 expression is associated with poor outcome in colorectal cancer (CRC). Whether the prognostic information is independent of known molecular subgroups and gene expression-based consensus molecular subtypes (CMS) is currently unknown. To investigate this, we analyzed nearly 2000 CRC biopsies and preclinical models. The expression of miR-31-5p and its host transcript, long noncoding RNA *MIR31HG*, was strongly correlated (Spearman's $\rho > 0.80$). *MIR31HG* outlier expression was observed in 158/1265 (12%) of pCRCs and was associated with depletion of CMS2-canonical subgroup (odds ratio = 0.21 [0.11–0.35]) and shorter relapse-free survival (RFS) in multivariable analysis (adjusted hazard ratio = 2.2 [1.6–3.0]). For stage II disease, 5-year RFS for patients with *MIR31HG* outlier status was 49% compared to 77% for those with normal-like expression. *MIR31HG* outlier status was associated with inferior outcome also within clinical high risk groups and within the poor prognostic CMS4-mesenchymal gene expression subtype specifically. Preclinical models with *MIR31HG* outlier expression were characterized by reduced expression of MYC targets as well as elevated epithelial-mesenchymal transition, TNF- α /NF κ B, TGF- β , and IFN- α / γ gene expression signatures, indicating cancer cell-intrinsic properties resembling the CMS4 subgroup—associations which were recapitulated in patient biopsies. Moreover, the prognostic value of *MIR31HG* outlier status was independent of cytotoxic T lymphocyte and fibroblast infiltration. We here present evidence that *MIR31HG* expression provides clinical stratification beyond major gene expression phenotypes and tumor immune and stromal cell infiltration and propose a model where increased expression is an indicator of a cellular state conferring intrinsic invasive and/or immuno-evasive capabilities.

Introduction

Colorectal cancer (CRC) patient classification according to the biologically distinct and gene expression-based consensus molecular subtypes (CMS) identifies a poor-prognostic CMS4-mesenchymal subgroup.¹ The value of CMS as a potential framework for stratified treatment is further

supported by emerging evidence of subtype-associated treatment responses.^{2–4} Bulk tumor gene expression profiles do however bear strong imprints of the sampled tumor microenvironment, and both immune infiltration and stromal abundance^{1,5} are correlated to CMS and provide interdependent prognostic information. Improved clinical precision is

Key words: colorectal cancer, biomarker, *MIR31HG*, miR-31-5p, gene expression profiles, consensus molecular subtypes

Abbreviations: CCLE: Cancer Cell Line Encyclopedia; CI: confidence interval; CIT: Cartes d'Identité des Tumeurs; CMS: consensus molecular subtypes; CRC: colorectal cancer; CRIS: CRC intrinsic subtypes; CTL: cytotoxic T lymphocyte; EMT: epithelial-mesenchymal transition; FDR: false discovery rate; FFPE: formalin fixed paraffin embedded; FPKM: fragments per kilobase of transcript per million mapped reads; GEO: Gene Expression Omnibus; HGU133p2: Affymetrix Human Genome U133 Plus 2.0; HR: hazard ratio; IFN: interferon; ISC: intestinal stem cell; lncRNA: long noncoding RNA; LICR: Ludwig Institute for Cancer Research; MAD: median absolute deviation; miRNA: microRNA; mCRC: metastatic colorectal cancer; MSI/MSS: micro-satellite instable/stable; mut: mutated; norm: normal; OR: odds ratio; pCRC: primary colorectal cancer; PDX: patient derived xenograft; qRT-PCR: real-time quantitative reverse transcription polymerase chain reaction; RPM: reads per million; RFS: relapse-free survival; TCGA: The Cancer Genome Atlas; wt: wild type

Additional Supporting Information may be found in the online version of this article.

Grant sponsor: Helse Sør-Øst RHF; **Grant sponsor:** Kreftforeningen; **Grant numbers:** 182759-20166824048-2016; **Grant sponsor:** Norges Forskningsråd; **Grant numbers:** 250993; **Grant sponsor:** Stiftelsen Kristian Gerhard Jebsen

DOI: 10.1002/ijc.31998

This is an open access article under the terms of the Creative Commons Attribution-NonCommercial License, which permits use, distribution and reproduction in any medium, provided the original work is properly cited and is not used for commercial purposes.

History: Received 12 May 2018; Accepted 31 Oct 2018; Online 17 Nov 2018

Correspondence to: Department of Molecular Oncology, Institute for Cancer Research, Oslo University Hospital, PO Box 4953 Nydalen, Oslo NO-0424, Norway; Tel.: 47-2278-1728, Fax: 47-2278-1745, E-mail: rlothe@tr-research.no

What's new?

Expression of miR-31 is associated with poor prognosis in colorectal cancer, but it's not known whether the prognostic value of the microRNA depends on consensus molecular subtypes (CMS). These authors looked at expression of *MIR31HG*, a long non-coding RNA derived from the same primary transcript as miR-31. They found that outlier expression of *MIR31HG* was associated with poor prognosis independent of CMS. Cells expressing high levels of *MIR31HG* also had strong enrichment for EMT and immune-related gene sets. The authors propose that *MIR31HG* outlier expression is a biomarker for pro-invasive and/or immunosuppressive characteristics, and poor prognosis.

dependent on identification of robust, independent markers with additional prognostic value.

MicroRNAs (miRNA) are ~22 nucleotide noncoding RNAs functioning as post-transcriptional gene repressors important in establishing and maintaining cell lineage identity.⁶ We have previously reported that miR-31-5p has oncogenic properties in CRC cell lines⁷ and in primary CRC (pCRC), elevated miR-31-5p expression has important clinicopathological and molecular associations, including advanced cancer stage, right-sided tumor localization, sessile serrated adenoma, low differentiation grade, micro-satellite instability (MSI) and mutated *BRAF* and *KRAS*.^{8,9} Furthermore, high expression levels have been associated with poor outcome in stage I–IV pCRCs.^{9,10}

Interestingly, and despite its clinicopathological and molecular associations, miR-31-5p expression has also been demonstrated to be independent of major gene expression subtypes.¹¹ Accordingly, we set out to (i) investigate the value of MIR31 as an independent prognostic marker in the context of gene expression subgroups and (ii) characterize intrinsic biological differences associated with MIR31 activity. Note that we here use the general term MIR31 to denote multiple RNA molecules encoded by the *MIR31HG* locus (previously known as *LncHIF-CAR* and *LOC554202*); *MIR31HG* long noncoding RNA (lncRNA) and the miR-31 hairpin precursor which through DGCR8/DROSHA/DICER1/XPO5 mediated processing and nuclear export gives rise to mature miR-31-5p and miR-31-3p conjugates. An outline of the present study is provided in Figure 1.

Materials and Methods

A total of 1993 samples were analyzed for MIR31 activity, including 129 preclinical models and 1854 pCRCs (not counting non-CRC cell lines and metastatic CRCs). In-house cell lines ($n = 35$) and patient samples ($n = 409$) were supplemented with publicly available gene expression data as outlined below and in Figure 1a.

RNA expression data and samples

Mature miR-31-5p and miR-31-3p expression was analyzed in small RNA sequencing data from CRC cell lines ($n = 29$ unique) and pCRCs ($n = 293$), as well as in qRT-PCR data from cell lines ($n = 59$). For analysis in larger sample sets and additional sample types, as well as of associations with gene expression signatures, the *MIR31HG* host gene was analyzed in gene-level expression data from the same cell lines and primary

CRCs, as well as additional cell lines ($n = 78$), patient-derived xenografts (PDXs, $n = 51$), pCRCs ($n = 1864$), normal colonic mucosa samples ($n = 41$), and metastatic CRCs ($n = 37$).

In-house CRC cell line ($n = 29$) Affymetrix Human Transcriptome Array 2.0 (HTA2.0) and small RNA-seq expression data have previously been published and are available from Gene Expression Omnibus (GEO) with accession identifier GSE97023 and in Supporting Information: Data 1, respectively.¹² The Cancer Genome Atlas (TCGA) level 3 RNA-seq RSEM gene-level ($n = 599$) and smRNA-seq RPM isoform-level data ($n = 293$) were downloaded from Broad GDAC Firehose with identifier doi:10.7908/C11G0KM9.¹³ Broad Cancer Cell Line Encyclopedia (CCLE) RNA-seq gene-level read count data ($n = 1,019$) were downloaded from <https://portals.broadinstitute.org/ccle/> (dated August 15, 2017).¹⁴ CRC PDX RNA-seq FPKM values ($n = 51$) were retrieved from Supplementary Table 1 in Ref. 15. NCI-60 cancer cell line ($n = 59$) qRT-PCR miRNA data were downloaded from <https://wiki.nci.nih.gov/display/NCIDTPdata> (accessed 2015-Mar-30).¹⁶ In-house pCRC ($n = 409$) and normal colonic mucosa ($n = 11$) Affymetrix Human Exon 1.0 ST and HTA2.0 microarray gene expression data have previously been published and are available from GEO with accession identifiers GSE24550, GSE29638, GSE69182, GSE79959, GSE97023 and GSE96528.² Normal colonic mucosa ($n = 31$) HTA2.0 gene expression will be submitted to GEO. Estevez-Garcia *et al.* Affymetrix Human Genome U133 Plus 2.0 (HGU133p2) metastatic CRC (mCRC) gene expression data ($n = 37$) were downloaded from GEO with accession identifier GSE52735.¹⁷ CCLE and Astra-Zeneca CRC cell line HGU133p2 were retrieved from GEO with accession identifiers GSE57083 [no reference] and GSE36133¹⁴ ($n = 28$ and $n = 17$ respectively, after exclusion of non-CRC and overlapping samples). Additional in-house HTA2.0 CRC cell line ($n = 6$) gene expression data will be submitted to GEO. Marisa *et al.* ($n = 566$) and Jorissen *et al.* ($n = 290$) HGU133p2 pCRC gene expression data were downloaded from GEO with accession identifiers GSE39582¹⁸ and GSE14333.¹⁹

Affymetrix microarray data were re-processed using the justRMA function in the R²⁰ package *affy*,²¹ with brainarray Entrez v20/v22 CDFs.²² ComBat method implemented in the R package *sva* was used to account for platform and batch effects.²³ For merging in-house, CCLE and Astra-Zeneca samples, the 13 replicated cell lines were included as covariates in the ComBat model matrix.

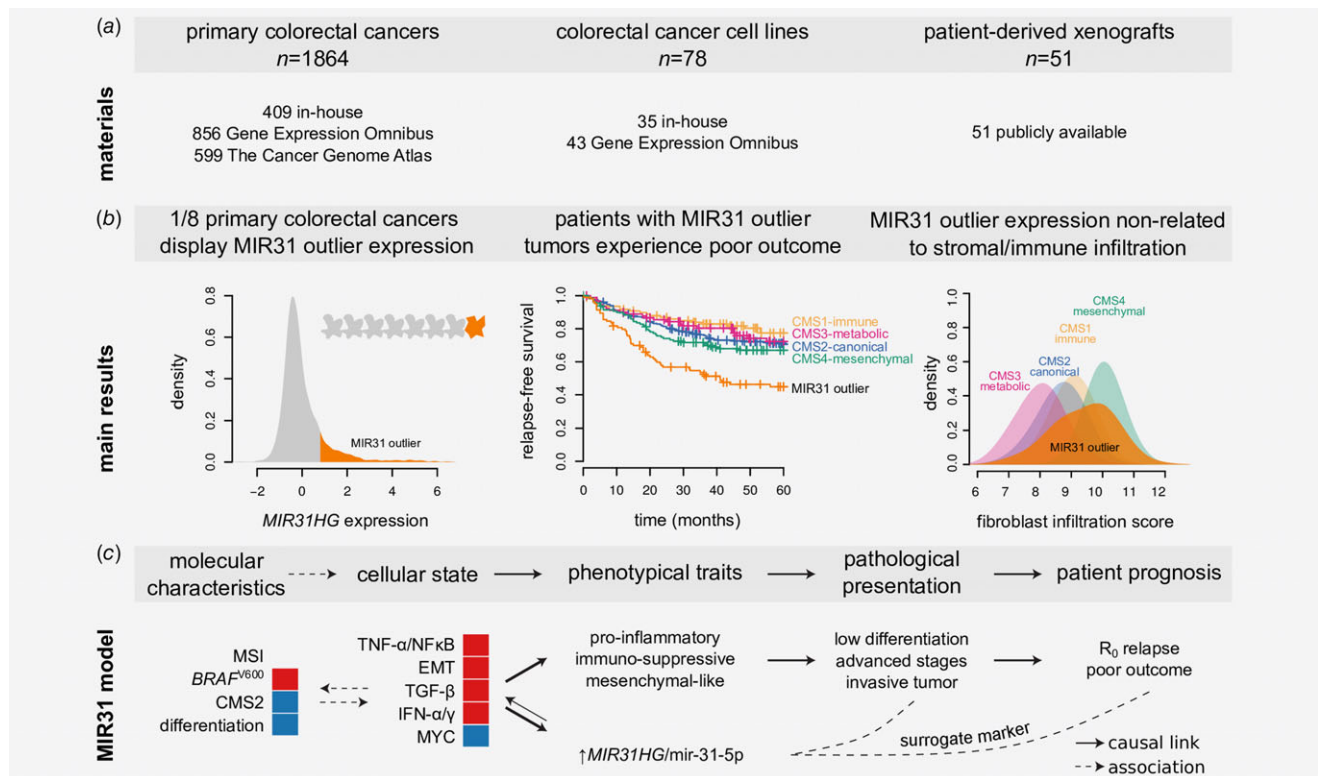


Figure 1. Study outline (a) Panel shows materials included with further details in the Methods section. (b) Panel illustrates the main results with further details in the Results section. (c) We propose a model where high *MIR31HG*/miR-31-5p expression is a surrogate marker of poor outcome by acting as marker of a cellular state defined by relative activation of epithelial-mesenchymal transition (EMT), TNF- α /NF κ B, TGF- β , and IFN- α/γ gene circuits as well as relative downregulation of MYC targets. This cellular state is causally related to acquisition of traits linked to immune evasion, invasion and/or metastasis. Red and blue indicate activation/enrichment and reduction/depletion, respectively. CMS: consensus molecular subtype; IFN: interferon; MSI: micro-satellite instable; R₀: tumor-free resection margin.

Additional cell line data

CRC cell line MSI and nonsynonymous *KRAS* (codons 12, 13, 61, 117 and 146), *BRAF* (codon 600), *TP53*, *DGCR8*, *DROSHA*, *DICER1* and *XPO5* mutation statuses were compiled mainly from <https://portals.broadinstitute.org/ccl/> (dated 2017-Aug-15),¹⁴ Supplementary Table 2 in Ref. 24, Supplementary Table 1 in Ref. 25 and <https://cancer.sanger.ac.uk/cosmic/download> (v84).²⁶ Tumor localization was determined from the primary papers describing cell line establishment and sites of origin proximal to the splenic flexure were set to right-sided (retrieved for 38/78 samples). Cell line annotations including Cellosaurus Research Resource Identifiers are available in Supporting Information: Data 1.

Gene expression-based classification of samples

MIR31HG expression was used to define *MIR31 outliers* as samples with expression higher than $median(x_{MIR31HG}) + 3 \times MAD(x_{MIR31HG})$ where $x_{MIR31HG}$ represents either 2^{\log_2} justRMA²¹ signal values (microarray) or normalized read values (sequencing) and *MAD* represents the corresponding within-dataset cross-sample median absolute deviation. Samples with *CDX2* expression below the 15.6% percentile in each dataset were classified as *CDX2* negative.²⁷ CMS labels for pCRCs from the CIT, LICR and TCGA (COADREAD) datasets

were retrieved from Sage Bionetworks Synapse (identifier syn4978511). pCRCs in the Oslo series were classified using the `classifyCMS.RF` function in the R package `CMSclassifier` with default posterior probability threshold.¹ CRC cell lines were classified according to CMS using `CMScaller`.²⁸ Cell line differentiation state was determined as previously described.¹² Classification of pCRCs according to the CRC intrinsic subtypes (CRIS)²⁹ was performed using `CMScaller` function in the R package `CMScaller`²⁸ with CRIS template genes from Supplementary Table 8 in Ref. 29. Samples with classification false discovery rate (FDR) > 0.05 were not assigned (n/a).

Differential expression analysis

Differential gene expression analysis was performed using `limma`.³⁰ Differential protein expression analysis was performed using Welch's test. Proteins with missing values were not considered.

Gene set analysis

Gene sets were preselected to be CRC and CMS-informative based on Guinney *et al.*¹ and are listed in Supporting Information: Data 2. Camera gene set analysis³¹ was performed using the R package `limma`.³⁰ Tumor cytotoxic T lymphocyte and fibroblast infiltration scores were calculated using the R package

MCPcounter.³² Normal colonic fibroblast TGF- β response signature was downloaded from Supplementary Table 8 in Ref. 5 and single sample gene set enrichment analysis scores calculated using the *gsa* function in the R package GSEA.³³ ABSOLUTE³⁴ tumor percentage estimates were retrieved from Supplementary Data 1 in Ref. 35.

Survival analysis

For survival analysis, three cohorts of pCRCs were merged (total $n = 1,265$). The in-house Norwegian Oslo series is a consecutive, population-based collection of biopsies from patients that received surgery for stage I–IV pCRCs between 2005 and 2013 ($n = 409$).² The French multi-center Cartes d'Identité des Tumeurs (CIT) is a cohort of stage I–IV colon cancers that underwent surgery between 1987 and 2007 ($n = 566$).¹⁸ The Australian/American Ludwig Institute for Cancer Research (LICR) dataset consists of stage I–IV pCRCs ($n = 290$).¹⁹ Information regarding approvals and patient consent are given in the referenced publications. Clinical annotation data were retrieved from the associated Gene Expression Omnibus (GEO) record. Baseline characteristics are presented in Supporting Information: Table S1.

Kaplan–Meier and Cox proportional hazard analyses were performed using the R package survival.³⁶ Specifically, hazard ratios (HR), 95% confidence intervals (CI) and Wald tests were calculated using the *coxph* function. Model output was formatted using the R package Greg.³⁷ The primary end-point in the prognostic analyses was five-year relapse-free survival where relapse, locally or distant, or death from any cause was registered as events. The secondary end-point was five-year overall survival. Death from any cause were registered as event and patients were censored at loss to follow-up, defined as last date of inquiry about death, or 5 years after surgery. R function *cutoff.survival* from Ref. 38 was used to estimate hazard ratios as a function of *MIR31HG* expression dichotomization threshold.

Cox model covariate inclusion was based on established associations with patient outcome, known association to miR-31-5p expression and data availability. Clinical stage and CMS were included as factorial covariates. Cox model proportional hazard assumption was tested using the *cox.zph* function and for covariates and models, p values were > 0.05 .

Additional statistical analysis

All presented p values are two-sided. Spearman's and Pearson's correlation, Fisher's Exact and Pearson's χ^2 tests were performed using functions *cor*, *fisher.test* and *chisq.test* in the R package stats. Cochran-Armitage test for trend was performed using the *chisq.test* function in the R package coin.³⁹

Results

Cancer cell-intrinsic MIR31HG/miR-31-5p outlier expression in colorectal cancers

To enable analysis of MIR31 expression in large gene-level datasets, strong expression correlation among the host gene

MIR31HG and both mature mir-31 conjugates, miR-31-5p and miR-31-3p, was confirmed in CRC cell lines¹² and primary tumors¹³ with matching RNA (microarrays or total RNA sequencing) and miRNA (small RNA sequencing) expression data (*MIR31HG*/miR-31-5p: Spearman's $\rho_{\text{cells}} = 0.80$ and $\rho_{\text{pCRC}} = 0.80$; miR-31-5p/miR-31-3p, Supporting Information: Fig. S1). For cell lines, *MIR31HG*/miR-31-5p correlation was slightly improved when samples carrying coding mutations in either of the *DGCR8/DROSHA/DICER1/XPO5* miRNA-processing genes were excluded ($\rho_{\text{wt}} = 0.82$, Supporting Information: Fig. S1a).

Cell line differences in both miR-31-5p and *MIR31HG* expression levels separately were recapitulated across laboratories and technological platforms indicating biological stability and analytical robustness (Supporting Information: Fig. S2a and b and text). Furthermore, comparison with cell lines from other cancer types indicated that CRC cell lines have a wide range of *MIR31HG* expression levels (Fig. 2a and Supporting Information: Fig. S2c). Specifically, extrapolating from a linear least squares regression model in qRT-PCR data, we estimated the miR-31-5p abundance to range from roughly 20 to 10,000 copies/cell across our 29 CRC cell lines (Supporting Information: Fig. S2a).

MIR31HG outlier expression was also observed among PDX models,¹⁵ which similarly to cell lines also lack a human tumor microenvironment, and in colorectal tumors with different microenvironments, including primary² and metastatic lesions¹⁷ ($n = 29, 51, 409$ and 37 respectively, Fig. 2b). In contrast, outlier expression was not observed in normal colonic mucosa samples ($n = 41$, Fig. 2a). This indicates that *MIR31HG* outlier expression is both cancer-specific and cancer cell-intrinsic, i.e. not attributable to infiltrating immune or stroma cells. In further support of this, paired pCRCs and PDXs⁴⁰ showed consistent expression levels; 3 out of 15 primary tumors and their paired xenografts showed highly elevated *MIR31HG* expression (Supporting Information: Fig. S3).

Taken together these data demonstrate that (i) miR-31-3p, miR-31-5p and *MIR31HG* expression levels are highly correlated, (ii) some CRC cell lines display high-level transcriptional upregulation of *MIR31HG*, which is recapitulated across technological platforms, research groups and conditions and (iii) a subset of primary and metastatic CRCs exhibit cancer cell-intrinsic *MIR31HG* outlier expression.

MIR31 outlier expression is an independent prognostic factor also within the CMS4-mesenchymal subgroup

To determine whether the clinicopathological and molecular stratifications of miR-31-5p expression also applies to *MIR31HG*, we merged three independent cohorts of totally 1,265 stage I–IV pCRCs; Oslo ($n = 409$),² CIT ($n = 566$, no rectum)¹⁸ and LICR ($n = 290$).¹⁹

MIR31HG expression distribution was heavily right-skewed with most samples having expression signals near the background levels, and a subset of 158/1265 (12%) having outlier

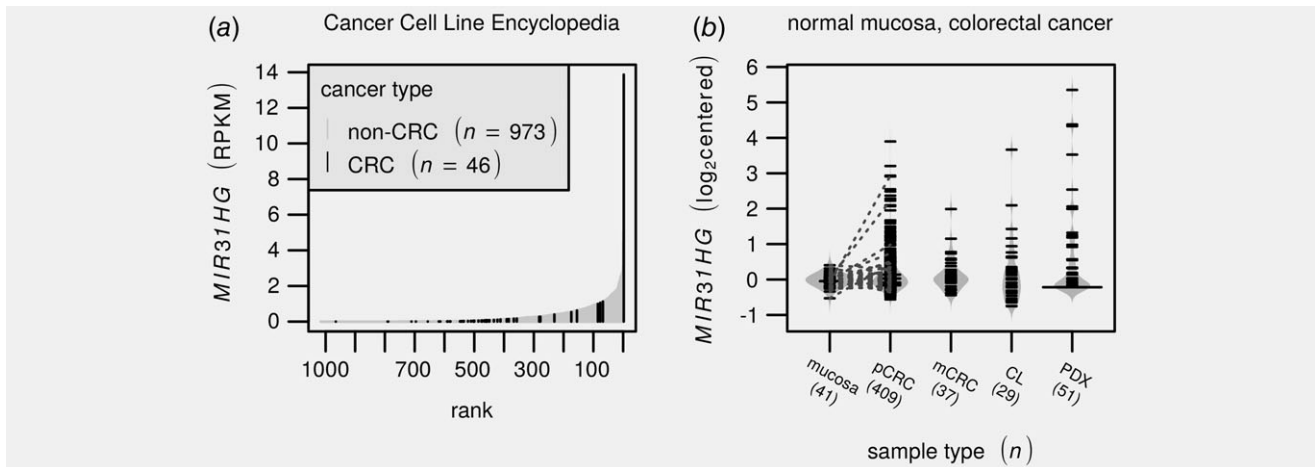


Figure 2. *MIR31HG* outlier expression is observed in a subset of primary colorectal cancers and derived preclinical models. (a) Barplot depicts *MIR31HG* expression across the Cancer Cell Line Encyclopedia¹⁴ with colorectal cancer samples highlighted in black. (b) Beanplot illustrates distributions in median centered *MIR31HG* expression estimates across normal colonic mucosa, primary² and metastatic¹⁷ lesions as well as cell line¹² and PDX¹⁵ models. Numbers below labels indicate the number of samples. Line segments indicate matched mucosa/tumor pairs. Notice that there are pairs where only the tumor show outlier expression. PDX values are based on RNA-sequencing while the remaining are from different Affymetrix expression arrays. CL: cell line; pCRC/mCRC; primary/metastatic colorectal cancer; PDX; patient-derived xenograft; RPKM: reads per kilobase per million.

expression determined as expression above median + 3 × MAD (Fig. 3a). Consistent with published data, *MIR31* outlier tumors were more likely to be of advanced cancer stages ($p = 8.2 \times 10^{-5}$, Cochran-Armitage test for trend, Fig. 3b), to be right-sided (OR = 2.4 [1.7–3.5], $p = 2.6 \times 10^{-7}$, Fisher's exact test, Fig. 3c), have a low differentiation level (OR = 2.5 [1.1–5.5], $p = 0.03$, status only available for the Oslo cohort) and harbor *BRAF*^{V600} mutations (OR = 2.8 [1.7–4.7], $p = 8.1 \times 10^{-5}$). Neither patient age, MSI-status, *KRAS* or *TP53* mutations were associated with *MIR31* outlier status ($p > 0.05$, Fig. 3c and Supporting Information: Fig. S4a). Notably, although, *MIR31* outlier status was independent of MSI ($p = 0.33$, Fisher's exact test), the average *MIR31HG* expression was slightly higher in MSI compared to MSS tumors (\log_2 fold-change = 0.27, Supporting Information: Fig. S4b).

To assess how sensitive survival analyses were to the necessarily arbitrary dichotomization, we applied CutOff Finder³⁸ to calculate the hazard ratio (HR) as a function of *MIR31HG* expression threshold with 5-year relapse-free survival (RFS) as endpoint (stages II and III, $n = 826$, Fig. 3d). Strikingly, the HR remained near-constant within the bulk of the expression distribution with an inflection point near the applied outlier boundary, concurrently supporting both the molecular distinctiveness and the clinical validity of the *MIR31HG*-based sample dichotomization. For patients with stage II tumors exhibiting an *MIR31* outlier profile 5-year RFS was 49% compared to 77% for those with normal-like *MIR31HG* expression (HR = 2.5 [1.8–3.3], $p < 10^{-8}$, Wald test for Cox model including stage and *MIR31* status, Fig. 3e). *MIR31* outlier status was associated with inferior outcome also when stratified by adjuvant chemotherapy (Fig. 3f, Supporting Information: Fig. S5). Among stage II + III experiencing distant relapse, *MIR31* outlier patients

performed significantly worse than those with *MIR31* normal-like cancers with 5-year RFS of 0% and 42%, respectively ($p = 0.0052$, Wald test, HR = 2.8 [1.4–5.6], Supporting Information: Table S4 and Supporting Information: Fig. S6a). For patients with a stage II/T4 tumor, *MIR31* outlier status was again associated with inferior outcome ($p = 0.035$, HR = 3.5 [1.1–11], Supporting Information: Fig. S6b). Overall, the negative prognostic association was seen in all three patient cohorts individually but did not reach statistical significance in the smallest sample set (Supporting Information: Fig. S7b).

Subgroup analysis among stage II + III tumors showed that *MIR31* outlier expression was associated with inferior outcome within each of the molecular subgroups MSS, *BRAF*^{wt}, *BRAF*^{mut}, *TP53*^{wt}, *TP53*^{mut}, *CDX2* positive and *CDX2* negative separately, as well as for right-sided and left-sided/rectum tumors separately (Supporting Information: Fig. S8). The trend was similar also in the MSI subgroup, but not statistically significant ($p = 0.17$). Importantly, the pattern of a poorer outcome associated with *MIR31HG* outlier expression was consistent using 5-year overall survival as the endpoint (Supporting Information: Fig. S9) and in the three individual cohorts separately (Supporting Information: Figs. S12 and S13).

Our primary objective was to determine whether the prognostic information captured by miR-31-5p/*MIR31HG* expression is independent of major gene expression subtypes represented by CMS.¹ CRCs with outlier expression were not enriched in the poor-prognostic CMS4-mesenchymal group, indicating CMS-independency (Fig. 3g). The proportion of *MIR31* outliers was largely similar in CMS1-immune, CMS3-epithelial/metabolic and CMS4-mesenchymal, although a strong depletion among CMS2-epithelial/canonical was evident (OR = 0.21 [0.11–0.35]). Kaplan–Meier analysis showed that

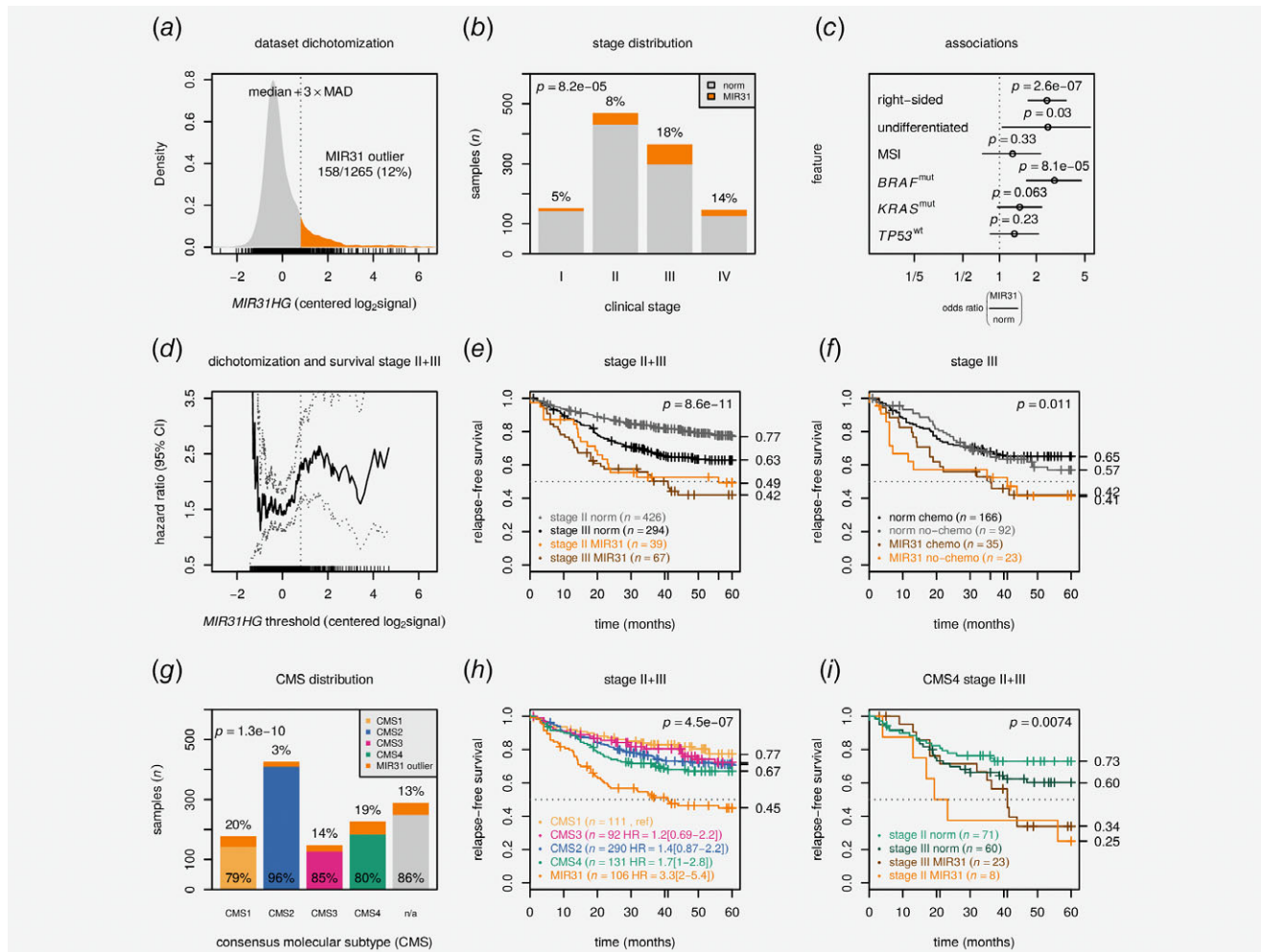


Figure 3. MIR31 outlier expression is a negative prognostic factor independent of consensus molecular subtypes. (a) Density plot shows centered *MIR31HG* expression and dichotomization threshold. (b) Barplot shows clinical stage and MIR31 outlier proportions. The p value is from a Cochran-Armitage test. (c) Plot visualizes odds ratios with 95% confidence intervals for selected clinicopathological and molecular variables. The p values are from Fisher's exact tests. Differentiation refers to low differentiation grade and was only available for 401 cases. (d) Univariable hazard ratio (HR) with 95% confidence interval is plotted as a function of *MIR31HG* threshold. Kaplan–Meier plots show relapse-free survival for (e) stage II + III pCRCs stratified according to stage and MIR31 status and (f) stage III pCRCs according to MIR31 status and adjuvant chemotherapy. The p values are from Wald tests for Cox models including stage (e) or chemo (f) in addition to MIR31 status. (g) Barplot illustrates distribution of CMS and MIR31 outliers. The p value is from χ^2 test. (h) Kaplan–Meier plot shows relapse-free survival for stage II + III pCRC patients stratified by CMS and MIR31 outlier status. The p value is from Wald test for a Cox model including only CMS/MIR31 status. (i) Kaplan–Meier plot shows relapse-free survival for CMS4 stage II + III pCRC patients stratified by MIR31 and stage. The p value is from Wald test for Cox model including stage and MIR31 status. Data are from CIT,¹⁸ LICR¹⁹ and Oslo² cohorts. HR: hazard ratio; MAD: median absolute deviation; mut: mutated; n/a: not assigned; MSI: micro-satellite instable.

tumors with *MIR31HG* outlier expression conferred a worse outcome compared to nonoutliers in all individual CMS group separately (Fig. 3h). Notably, within CMS4, stage II MIR31 outliers were associated with a worse outcome than stage III samples with nonoutlier *MIR31HG* expression (Fig. 3i). In multivariable analysis the prognostic value of MIR31 status was independent of *BRAF*^{V600}, CMS and tumor stage (multivariable HR = 2.2 [1.6–3.0], $p = 4.4 \times 10^{-6}$, Supporting Information: Table S2). The same pattern of high *MIR31HG* expression and poor outcome was apparent also when *MIR31HG* was treated as a continuous covariate ($p = 4.3 \times 10^{-5}$, Supporting Information:

Table S3) and with CRC intrinsic subtypes (CRIS)²⁹ in place of CMS (Supporting Information: Fig. S14).

Taken together, these data demonstrate that miR-31-5p and *MIR31HG* expression provide similar clinical association and that *MIR31HG* is a prognostic factor independent of CMS and other molecular subgroups of CRC.

MIR31 outlier expression is associated with cancer cell-intrinsic TGF- β , TNF- α /NF- κ B and IFN- α / γ signaling

To investigate the biological basis for the CMS-independent poor prognostic association, cancer-cell intrinsic characteristics

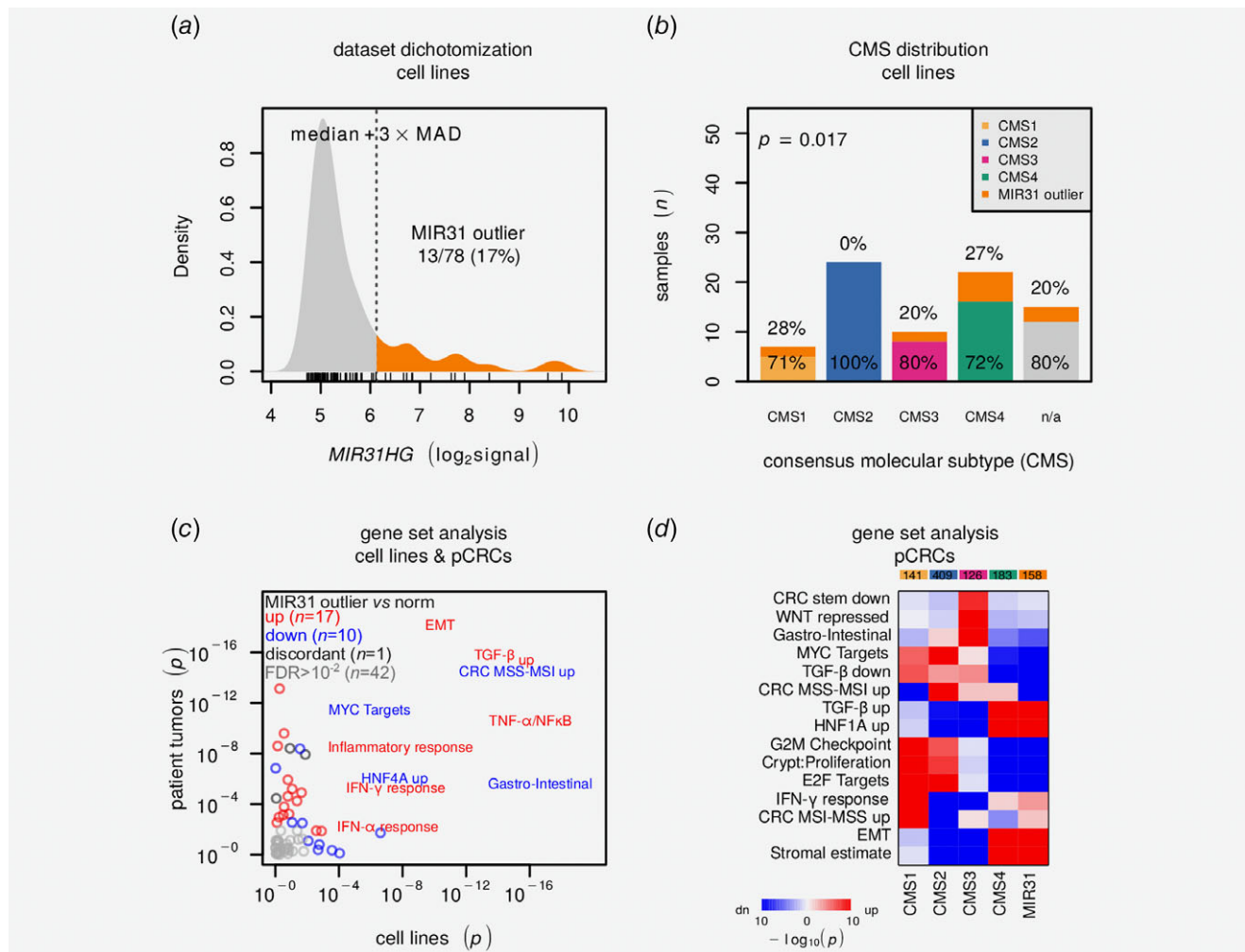


Figure 4. CRC cell line *MIR31HG* outlier expression is associated with differentiation state and immune-related signatures. (a) Density plot visualizes *MIR31HG* expression distribution with dichotomization threshold. (b) Barplot illustrates distribution of CMS and *MIR31* outliers. p Value is from χ^2 test. (c) Scatter plot visualizes gene set comparison of *MIR31* outliers against remaining samples for cell lines (horizontal) and patient tumors (vertical). p Values are from Camera³¹ test and red and blue indicate relative up- and downregulation. Gene sets with $FDR > 0.01$ in both cell lines and pCRCs are labeled. Further details are available in Supporting Information: Data 2. (d) Heatmap visualizes results from Camera³¹ gene set analysis comparing CMS and *MIR31* outliers. Color saturation indicates increasing significance and red and blue relative up- and downregulation, respectively. pCRC data are from CIT,¹⁸ LICR¹⁹ and Oslo² cohorts. CMS: consensus molecular subtypes; EMT: epithelial-mesenchymal transition; FDR: false discovery rate; IFN α /G: interferon- α / γ ; MAD: median absolute deviation; MSS/MSI: microsatellite stable/instable; pCRC; primary colorectal cancer; TGF β : transforming growth factor- β .

of *MIR31* outlier expression was assessed in a panel of CRC cell lines ($n = 78$) recapitulating the clinicopathological and molecular associations of *MIR31* outlier expression observed in the primary CRCs (Fig. 4a and b and Supporting Information: Fig. S15).

There was no significant overall depletion of predicted miR-31-5p target transcripts in *MIR31* outlier samples, neither at the mRNA nor the protein-level (Supporting Information: Fig. S17a and b). However, by Camera³¹ gene set analysis of 70 preselected CMS and CRC informative gene sets²⁸ (Fig. 4c), *MIR31* outlier cell lines were found to show strong enrichment for epithelial-mesenchymal transition (EMT) and immune-related gene sets such as TGF- β , TNF-

α /NF κ B and IFN- α / γ , as well as downregulation of MYC and HNF4A target genes (false discovery rate (FDR) adjusted $p < 0.005$). The *MIR31HG* locus lies within a ~ 300 kbp segment on chromosome 9 that encompasses most of the human repertoire of interferon genes (Supporting Information: Fig. S18a), and activation of interferon response in *MIR31* outliers was validated by collection of an independent set of nonoverlapping genes induced by IFN- α (Supporting Information: Fig. S18b). Critically, similar patterns were observed also for the pCRCs cohorts ($n = 1864$, total) and PDXs ($n = 51$)¹⁵ (Fig. 4c and Supporting Information: Data 2).

To further investigate the biological basis for the CMS-independent poor prognostic value of *MIR31* outlier

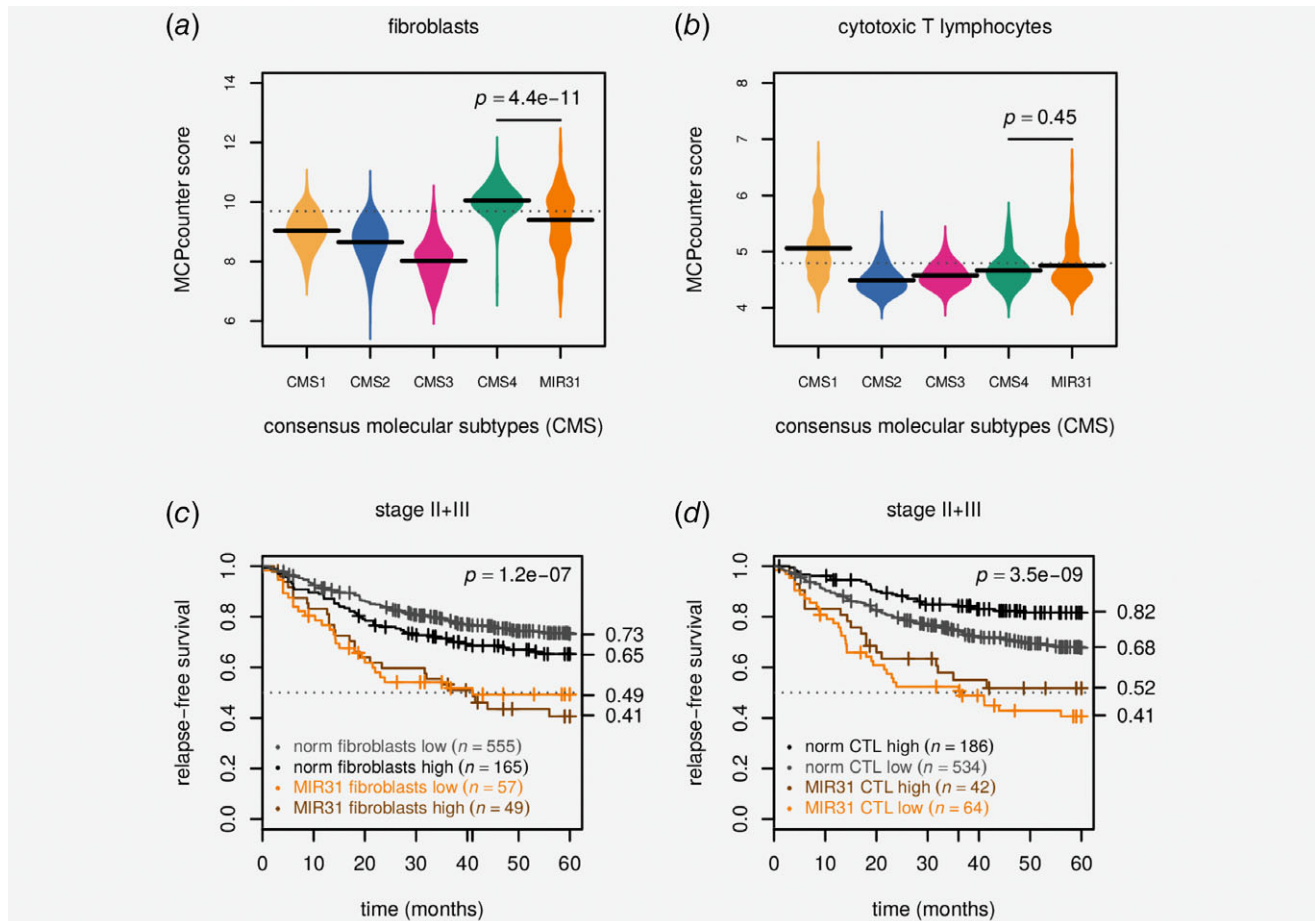


Figure 5. Poor prognostic value of MIR31 outlier expression is independent of cytotoxic lymphocyte and stromal infiltration. (a) Beanplot shows MCPcounter³² scores for fibroblasts and (b) cytotoxic T lymphocyte infiltration stratified by CMS and MIR31 outlier expression. The horizontal bars are the group-wise medians and the p values are from Wilcoxon rank sum tests. (c) Kaplan–Meier plot shows survival stratified by MIR31 and MCPcounter fibroblasts and (d) cytotoxic T lymphocyte scores. Both were dichotomized according to the 75th percentiles which are indicated with dashed horizontal lines in panels c and d. The p values are for Wald tests for the Cox models including MIR31 status in addition to either MCPcounter score. Data are from CIT,¹⁸ LICR¹⁹ and Oslo² cohorts. CTL: cytotoxic T lymphocyte.

expression, gene set analyses were performed in the context of CMS. Comparison of all MIR31 outliers (irrespective of CMS) with nonoutliers in each of the four CMS groups, showed that MIR31 outliers appeared biologically most similar to CMS4-mesenchymals (Fig. 4d and Supporting Information Fig. S19).

In conclusion, MIR31 outliers have intrinsic gene expression profiles associated with aggressive disease (undifferentiated state/EMT) and immune-associated signaling.

Poor prognostic value of MIR31 outlier expression is independent of stromal and cytotoxic lymphocyte infiltration

Considering that infiltration of stromal cells is both a marker of aggressiveness and a dominating feature of CMS4 tumors, stromal compositions were assessed in both the merged CIT + LICR+Oslo dataset ($n = 1,265$) and the TCGA pCRC cohort ($n = 599$)¹³ (representing different analytical platforms, microarrays and total RNA sequencing, respectively).

Quantification of fibroblasts specifically, based on gene expression (MCPcounter³²), showed that MIR31 outlier tumors had less fibroblast infiltration than CMS4 nonoutlier tumors in both datasets ($p < 10^{-8}$, Wilcoxon rank sum tests, Fig. 5a and Supporting Information: Fig. S20a). Similarly, for TCGA, DNA copy number-based ABSOLUTE³⁴ estimates indicated that tumors with MIR31 outlier expression had less infiltration of nonmalignant cells than nonoutlier tumors in both CMS4 and CMS1 (Supporting Information: Fig. S20b). Together, this suggests that the poor prognostic value of MIR31 is not predominantly attributable to stromal infiltration, supporting the prognostic independence from CMS.

In light of the many immune-related signatures with differential activation in MIR31 outliers, and the strong positive prognostic value of activated immune cells in CRC, we wanted to determine whether the poor prognosis of MIR31 outliers within the CMS4 subgroup could be explained by lower levels of cytotoxic T lymphocyte (CTL) infiltration. Gene expression-based

CTL quantification showed that the CTL infiltration was not significantly higher in CMS4 MIR31 outliers compared to CMS4 nonoutliers in neither the CIT+LICR+Oslo nor the TCGA datasets ($p > 0.1$, Wilcoxon rank sum test, Fig. 5b and Supporting Information: Fig. S21c).

Finally, survival analysis showed that the prognostic value of MIR31 was independent of both fibroblasts and CTL infiltration (Fig. 5c and d). For the stage II + III pCRCs in the three cohorts stratified by the 75th-percentile of fibroblast infiltration, RFS at 5-years were 73%/65% for MIR31 normal-like samples with fibroblasts high/low versus 49%/41% for MIR31 outliers fibroblasts high/low ($p < 0.001$). Similarly, for CTL stratified by the 75th-percentile, RFS at 5-years were 82%/68% for MIR31 normal-like samples with CTL high/low versus 52%/41% for MIR31 outlier samples with CTL high/low ($p < 0.001$), indicating that the cancer cell-intrinsic properties of tumors with MIR31 outlier expression conferred additive prognostic value to these well-known prognostic factors in CRC.

Discussion

High miR-31-5p expression has previously been established as a poor prognostic factor in pCRC.^{9,10} Here we provide evidence that MIR31 is a high-risk biomarker beyond known molecular subgroups, major gene expression phenotypes as well as tumor immune and stromal cell infiltration. Specifically, *MIR31HG* outlier expression identifies a subset of largely non-CMS2-canonical CRCs that show inferior outcome, also when controlling for clinicopathological and molecular factors, including but not limited to stage and *BRAF* mutations. The biological characteristics associated with MIR31 outlier expression were cancer cell-intrinsic, and we propose that miR-31-5p/*MIR31HG* expression is a marker of a cellular state conferring intrinsic pro-invasive and/or immuno-suppressive capabilities (Fig. 1c).

It has been shown that CRC organoids and cell line models exposed to either TGF- β or TNF- α undergo EMT with concomitant miR-31-5p induction, and TGF- β and TNF- α in combination act synergistically to increase miR-31-5p expression.⁴¹ It is therefore tempting to speculate that elevated *MIR31HG* is a surrogate marker of dual activation of TGF- β and TNF- α /NF κ B related signaling. These circuits confer intrinsic immune evasive and tissue invasive capabilities and may as such provide the biological basis for the aggressive disease associated with *MIR31HG* outlier expression. Corroborating this, CRC cell lines, PDXs and primary tumors with MIR31 outlier profile were characterized by reduced differentiation (EMT) and relative upregulation of gene signatures related to TNF- α /NF κ B, TGF- β , IFN- α and IFN- γ signaling, as well as downregulation of MYC targets. TGF- β suppression is critical in intestinal differentiation⁴² and is in the CRC-setting associated with metastatic capabilities⁴³ and tumor T-cell exclusion.⁴⁴ MIR31 outlier expression was not associated with T-cell exclusion in our study, however, interferons are

known to be produced by most cell types and modulate cancer immune surveillance. The gene set analyses therefore suggest that the poor prognostic value of high *MIR31HG* expression is partly linked to intrinsic immune modulatory signaling and/or resistance. In a recent study investigating the interplay between the colonic mucosa and immune system in colitis, it was found that intestinal epithelium miR-31-5p expression was strongly upregulated in colitis models induced by either IL10-knockout or chemical treatment, and miR-31-5p expression was also significantly higher in inflamed compared to normal mucosa from Crohn's patients.⁴⁵ Thus, intestinal epithelial miR-31-5p expression seems intrinsically linked to colonic inflammation—known to increase the risk of developing CRC. Alternatively, the poor outcome associated with high MIR31 activity may be related to the role of miR-31-5p in promoting stem cell expansion.⁴⁶ MIR31 positivity may represent stem cell-like subpopulations inherently resistant to chemotherapy, and LGR5⁺ positive stem cells were recently found to be critical in the formation and maintenance of CRC liver metastasis.⁴⁷ In this context, it is interesting to note that in patients with stage III CRC and MIR31 outlier expression, adjuvant chemotherapy did not appear to improve the patient outcome.

It has recently been reported that high miR-31-3p expression is also associated with resistance to anti-EGFR treatment in *KRAS* wild-type metastatic CRCs.⁴⁸ This is consistent with the finding that MIR31 outliers are depleted of CMS2-canonical cases, considering earlier work from us and others showing that transit-amplifying/CMS2-like preclinical models show the highest sensitivity toward EGFR inhibition.^{2,25} We speculate that patients with CRC exhibiting MIR31 outlier profile may present a particularly important clinical subgroup, with intrinsic aggressiveness combined with resistance toward standard chemotherapeutics and targeted treatment. The large variation in *MIR31HG*/miR-31-3p/miR-31-5p expression indicates that they represent analytically robust biomarkers, and *in situ* hybridization or qRT-PCR based diagnostic tests may be readily implementable.

For bulk tumor tissue samples, heterogeneity in sample composition introduces noise and *MIR31HG* may, with its large dynamic range and on/off-like expression pattern, provide a clean and robust readout. Although *MIR31HG* outlier profiles were shown to be both cancer-specific and cancer cell-intrinsic, we cannot exclude the possibility that the non-cancerous tumor compartment may contribute to *MIR31HG* expression in some cases. Recently, it was shown that miR-31-5p expression in T cells increased during exposure to type I interferons.⁴⁹ However, our analyses indicated that the prognostic value of MIR31 was independent of the level of CTL infiltration, and combination of the two markers identified a patient subgroup with a particularly poor survival.

To further characterize the role of MIR31 in CRC, the presented MIR31 outlier cell lines provide ideal models for knock-out experiments. It would be particularly interesting to

follow-up on two recent reports. Shih *et al.* showed that *MIR31HG*, independent of the encoded miR-31-5p, promotes tumor development through HIF1A co-activation.⁵⁰ Tian and colleagues demonstrated that miR-31-5p acts as a “cell-autonomous post-transcriptional regulator of the ISC [intestinal stem cell] niche” and is induced upon tissue damage by facilitating the subsequent expansion of LGR5⁺ ISCs as to repopulate the intestinal lining.⁴⁶

We provide evidence that *MIR31* carries prognostic information beyond consensus molecular subtypes and *MIR31* outlier status defines a subset of patients with inferior outcome

even within the CMS4-mesenchymal patient group. A bio-clinical model is proposed: miR-31-5p/*MIR31HG* outlier expression is a biomarker of a cellular state conferring cancer cell-intrinsic pro-invasive and/or immuno-suppressive capabilities resulting in poor patient prognosis.

Acknowledgements

We are grateful to Professor Arild Nesbakken at the Department of Gastroenterological Surgery, Oslo University Hospital, for generously making the detailed and quality controlled clinical annotations for the Oslo cohort available to our study.

References

- Guinney J, Dienstmann R, Wang X, et al. The consensus molecular subtypes of colorectal cancer. *Nat Med* 2015;21:1350–6.
- Sveen A, Bruun J, Eide PW, et al. Colorectal cancer consensus molecular subtypes translated to preclinical models uncover potentially targetable cancer cell dependencies. *Clin Cancer Res* 2018;24:794–806.
- Song N, Pogue-Geile KL, Gavin PG, et al. Clinical outcome from oxaliplatin treatment in stage II/III colon cancer according to intrinsic subtypes: secondary analysis of NSABP C-07/NRG oncology randomized clinical trial. *JAMA Oncol* 2016;2:1162–9.
- Okita A, Takahashi S, Ouchi K, et al. The consensus molecular subtypes of colorectal cancer as a predictive factor for chemotherapies against metastatic colorectal cancer. *JCO* 2018;36:736–6.
- Calon A, Lonardo E, Berenguer-Llargo A, et al. Stromal gene expression defines poor-prognosis subtypes in colorectal cancer. *Nat Genet* 2015;47:320–9.
- Ebert MS, Sharp PA. Roles for MicroRNAs in conferring robustness to biological processes. *Cell* 2012;149:515–24.
- Cekaite L, Rantala JK, Bruun J, et al. MiR-9, -31, and -182 deregulation promote proliferation and tumor cell survival in colon cancer. *Neoplasia* 2012;14:868–79.
- Schee K, Boye K, Abrahamsen TW, et al. Clinical relevance of microRNA miR-21, miR-31, miR-92a, miR-101, miR-106a and miR-145 in colorectal cancer. *BMC Cancer* 2012;12:505.
- Nosho K, Igarashi H, Nojima M, et al. Association of microRNA-31 with *BRAF* mutation, colorectal cancer survival and serrated pathway. *Carcinogenesis* 2014;35:776–83.
- Slattery ML, Pellatt AJ, Lee FY, et al. Infrequently expressed miRNAs influence survival after diagnosis with colorectal cancer. *Oncotarget* 2017;8:83845–59.
- Cantini L, Isella C, Petti C, et al. MicroRNA-mRNA interactions underlying colorectal cancer molecular subtypes. *Nat Commun* 2015;6:8878.
- Berg KCG, Eide PW, Eilertsen IA, et al. Multi-omics of 34 colorectal cancer cell lines - a resource for biomedical studies. *Mol Cancer* 2017;16:116.
- TCGA. Comprehensive molecular characterization of human colon and rectal cancer. *Nature* 2012;487:330–7.
- Barretina J, Caponigro G, Stransky N, et al. The cancer cell line encyclopedia enables predictive modelling of anticancer drug sensitivity. *Nature* 2012;483:603–307.
- Gao H, Korn JM, Ferretti S, et al. High-throughput screening using patient-derived tumor xenografts to predict clinical drug response. *Nat Med* 2015;21:1318–25.
- Gaur A, Jewell DA, Liang Y, et al. Characterization of MicroRNA expression levels and their biological correlates in human cancer cell lines. *Cancer Res* 2007;67:2456–68.
- Estevez-Garcia P, Rivera F, Molina-Pinelo S, et al. Gene expression profile predictive of response to chemotherapy in metastatic colorectal cancer. *Oncotarget* 2015;6:6151–9.
- Marisa L, De Reyniès A, Duval A, et al. Gene expression classification of colon cancer into molecular subtypes: characterization, validation, and prognostic value. *PLoS Med* 2013;10:e1001453.
- Jorissen RN, Gibbs P, Christie M, et al. Metastasis-associated gene expression changes predict poor outcomes in patients with dukes stage B and C colorectal cancer. *Clin Cancer Res* 2009;15:7642–51.
- R Core Team. *R: a language and environment for statistical computing*. Vienna, Austria: R Foundation for Statistical Computing, 2018.
- Gautier L, Cope L, Bolstad BM, et al. Affy—analysis of Affymetrix GeneChip data at the probe level. *Bioinformatics* 2004;20:307–15.
- Sandberg R, Larsson O. Improved precision and accuracy for microarrays using updated probe set definitions. *BMC Bioinform* 2007;8:1.
- Leek JT, Scharpf RB, Bravo HC, et al. Tackling the widespread and critical impact of batch effects in high-throughput data. *Nat Rev Genet* 2010;11:733–9.
- Mouradov D, Sloggett C, Jorissen RN, et al. Colorectal cancer cell lines are representative models of the main molecular subtypes of primary cancer. *Cancer Res* 2014;74:3238–47.
- Medico E, Russo M, Picco G, et al. The molecular landscape of colorectal cancer cell lines unveils clinically actionable kinase targets. *Nat Commun* 2015;6:7002.
- Iorio F, Knijnenburg TA, Vis DJ, et al. A landscape of pharmacogenomic interactions in cancer. *Cell* 2016;166:740–54.
- Pilati C, Taieb J, Balogoun R, et al. CDX2 prognostic value in stage II/III resected colon cancer is related to CMS classification. *Ann Oncol* 2017;28:1032–5.
- Eide PW, Bruun J, Lothe RA, et al. CMScaller: an R package for consensus molecular subtyping of colorectal cancer pre-clinical models. *Sci Rep* 2017;7:16618.
- Isella C, Brundu F, Bellomo SE, et al. Selective analysis of cancer-cell intrinsic transcriptional traits defines novel clinically relevant subtypes of colorectal cancer. *Nat Commun* 2017;8:ncomms15107.
- Ritchie ME, Phipson B, Wu D, et al. Limma powers differential expression analyses for RNA-sequencing and microarray studies. *Nucl Acids Res* 2015;43:e47.
- Wu D, Smyth GK. Camera: a competitive gene set test accounting for inter-gene correlation. *Nucl Acids Res* 2012;40:e133.
- Becht E, Giraldo NA, Lacroix L, et al. Reyniès a de. Estimating the population abundance of tissue-infiltrating immune and stromal cell populations using gene expression. *Genome Biol* 2016;17:218.
- Hänzelmann S, Castelo R, Guinney J. GSVA: gene set variation analysis for microarray and RNA-seq data. *BMC Bioinformatics* 2013;14:7.
- Carter SL, Cibulskis K, Helman E, et al. Absolute quantification of somatic DNA alterations in human cancer. *Nat Biotechnol* 2012;30:413–21.
- Aran D, Sirota M, Butte AJ. Systematic pan-cancer analysis of tumour purity. *Nat Commun* 2015;6:8971.
- Therneau TM. A package for survival analysis in S. 2015.
- Gordon M, Seifert R. *Greg: Regression helper functions*. 2016
- Budczies J, Klauschen F, Sinn BV, et al. Cutoff finder: a comprehensive and straightforward web application enabling rapid biomarker cutoff optimization. *PLoS One* 2012;7:e51862.
- Hothorn T, Hornik K, van De Wiel MA, et al. Implementing a class of permutation tests: the coin package. *J Stat Softw* 2008;28:1–23.
- Linnekamp JF, van Hooft SR, Prasetyanti PR, et al. Consensus molecular subtypes of colorectal cancer are recapitulated in *in vitro* and *in vivo* models. *Cell Death Differ* 2018;25:616–33.
- Cottonham CL, Kaneko S, Xu L. miR-21 and miR-31 converge on TIAM1 to regulate migration and invasion of colon carcinoma cells. *J Biol Chem* 2010;285:35293–302.
- Reynolds A, Wharton N, Parris A, et al. Canonical WNT signals combined with suppressed TGFβ/BMP pathways promote renewal of the native human colonic epithelium. *Gut* 2014;63:610–21.
- Calon A, Espinet E, Palomo-Ponce S, et al. Dependency of colorectal cancer on a TGF-

- β -driven programme in stromal cells for metastasis initiation. *Cancer Cell* 2012;22:571–84.
44. Tauriello DVF, Palomo-Ponce S, Stork D, et al. TGF β drives immune evasion in genetically reconstituted colon cancer metastasis. *Nature* 2018;554:538–43.
 45. Shi T, Xie Y, Fu Y, et al. The signaling axis of microRNA-31/interleukin-25 regulates Th1/Th17-mediated inflammation response in colitis. *Mucosal Immunol* 2017;10:983–95.
 46. Tian Y, Ma X, Lv C, et al. Stress responsive miR-31 is a major modulator of mouse intestinal stem cells during regeneration and tumorigenesis. *Elife* 2017;6:e29538.
 47. De Sousa e Melo F, Kurtova AV, Harnoss JM, et al. A distinct role for Lgr5+ stem cells in primary and metastatic colon cancer. *Nature* 2017;543:676–80.
 48. Pugh S, Thiébaud R, Bridgewater J, et al. Association between miR-31-3p expression and cetuximab efficacy in patients with *KRAS* wild-type metastatic colorectal cancer: a post-hoc analysis of the new EPOC trial. *Oncotarget* 2017;8: 93856–66.
 49. Moffett HF, Cartwright ANR, Kim H-J, et al. The microRNA miR-31 inhibits CD8+ T cell function in chronic viral infection. *Nat Immunol* 2017;18: 791–9.
 50. Shih J-W, Chiang W-F, Wu ATH, et al. Long noncoding RNA *LncHIFCAR/MIR31HG* is a HIF-1A co-activator driving oral cancer progression. *Nat Commun* 2017;8:15874.